Separate and combined effects of *Sod1* and *Cdh23* mutations on age-related hearing loss and cochlear pathology in C57BL/6J mice

Kenneth R. Johnson[a,*], **Heping Yu**[a,b], **Dalian Ding**[c], **Haiyan Jiang**[c], **Leona H. Gagnon**[a], and **Richard J. Salvi**[c]

[a] The Jackson Laboratory, Bar Harbor, ME 04609

[c] Center for Hearing and Deafness, State University of New York, Buffalo, NY 14214

Abstract

Both the *ahl* allele of *Cdh23* and the null mutation of *Sod1* have been shown to contribute to age-related hearing loss (AHL) in mice, but mixed strain backgrounds have confounded analyses of their individual and combined effects. To test for the effects of *Sod1* deficiency independently from those of $Cdh23^{ahl}$, we produced mice with four digenic genotypes: $Sod1^{+/+}Cdh23^{ahl/ahl}$, $Sod1^{+/+} Cdh23^{+/+}$, $Sod1^{-/-} Cdh23^{ahl/ahl}$, and $Sod1^{-/-} Cdh23^{+/+}$, all on a uniform C57BL/6J strain background. We assessed hearing loss by ABR threshold measurements and evaluated cochlear pathologies in age-matched mice of each digenic combination. ABR analysis showed that $Sod1^{+/+} Cdh23^{+/+}$ mice retain normal hearing up to 15 months of age and that hearing loss of $Sod1^{+/+} Cdh23^{ahl/ahl}$ mice is more age and frequency dependent than that of $Sod1^{-/-} Cdh23^{+/+}$ mice. ABR results also showed that mice with both gene mutations ($Sod1^{-/-} Cdh23^{ahl/ahl}$) exhibit the earliest onset and most severe hearing loss, greater than predicted for strictly additive effects. Histological analysis of cochleas showed that hair cell lesions are most severe in $Sod1^{-/-} Cdh23^{ahl/ahl}$ mice followed closely by $Sod1^{+/+} Cdh23^{ahl/ahl}$ mice and much smaller in $Sod1^{-/-} Cdh23^{+/+}$ and $Sod1^{+/+} Cdh23^{+/+}$ mice. Despite extensive damage to cochlear hair cells, vestibular hair cells appeared remarkably normal in all strains. Although both $Sod1^{-/-}$ and $Cdh23^{ahl/ahl}$ genotypes had strong effects on hearing loss, the $Cdh23^{ahl/ahl}$ genotype was primarily responsible for the increase in hair cell loss, suggesting that the two mutations have different underlying mechanisms of pathology.

Keywords

age-related hearing loss; *Sod1*; *Cdh23*; *ahl*; C57BL/6J; inbred mouse strain; cochlear pathology; ABR thresholds

1. Introduction

Age-related hearing loss (AHL) or presbycusis is a major health concern because of its widespread occurrence among the elderly and its negative influence on their quality of life

*Corresponding author. phone: 207-288-6228, fax: 207-288-6149, ken.johnson@jax.org.
[b]Present address: Case Western Reserve University, Cleveland, OH

(Dalton et al., 2003). AHL can be exacerbated by a variety of environmental insults including exposures to loud noises and ototoxic drugs, but at its core is a significant genetic component (DeStefano et al., 2003). Recently, an extensive whole genome association study identified the first human gene mutation that confers susceptibility to AHL (Friedman et al., 2009), but genetic studies of complex traits in human populations remain difficult undertakings. Laboratory strains of mice offer important advantages for studying the genetic basis for AHL because of their short life span, well-defined genetics, and the ability to control their environment. The C57BL/6J strain of mice, in particular, has been used extensively as a model for AHL (Henry et al., 1980; Hequembourg et al., 2001; Mikaelian, 1979; Wang et al., 2008; Willott, 1986). Hearing loss in these mice is first detected in the high frequencies as early as 3–6 months of age (Spongr et al., 1997) and progresses to severe impairment by one year of age (Zheng et al., 1999).

To map genes that might underlie AHL in C57BL/6J (B6) mice, a linkage backcross was generated with mice of the wild-derived inbred strain CAST/EiJ (CAST), which retain normal hearing to old age. Analysis of this cross detected a locus on mid-Chromosome 10 that showed a highly significant linkage with the auditory brainstem response (ABR) thresholds of backcrossed mice (Johnson et al., 1997), and the recessive hearing loss susceptibility allele of this locus, derived from the B6 parent, was designated *ahl*. The same Chr 10 locus was shown to contribute to AHL in several other inbred mouse strains (Johnson et al., 2000), and subsequent evidence indicated that the strains share the same *ahl* allele, which is a splice variant of the cadherin 23 (*Cdh23*) gene (Noben-Trauth et al., 2003). To evaluate the isolated effect of this variant on AHL, a congenic strain, designated B6.CAST-*Cdh23^{Ahl+}*/Kjn, was produced by backcrossing the CAST-derived AHL resistance allele (*Ahl+*) onto the B6 strain background. The congenic mice were shown to be protected from early onset hearing loss and basal turn hair cell degeneration, but older mice showed a moderate degree of hearing loss and ganglion cell degeneration, which was greater than that seen in CAST mice but less than that observed in B6 mice (Keithley et al., 2004). Cadherin 23 (CDH23), the protein encoded by *Cdh23*, later was shown to be a component of stereocilia tip links, which are thought to gate mechanotransduction channels in hair cells (Kazmierczak et al., 2007). The *ahl* variant of *Cdh23*, like a recently described ENU-induced missense mutation of this gene (Schwander et al., 2009), may encode a defective protein that weakens tip links or impedes their repair. The accumulation of broken tip links over time could explain the progressive hearing loss associated with these variant alleles.

Oxidative stress and free radical production have also been shown to contribute to AHL in inbred mouse strains (Jiang et al., 2007; McFadden et al., 2001; Staecker et al., 2001). Normal cellular respiration results in the production of the highly toxic superoxide radical that damages cells if it is not quickly eliminated. The superoxide radical is normally eliminated from cells by a family of superoxide dismutase (SOD) enzymes, the most abundant of which is Cu/Zn SOD. Cu/Zn SOD, coded by the *Sod1* gene, is abundantly expressed in the cochlea and plays a key role in reducing oxidative stress. Inactivation of the *Sod1* gene was reported to accelerate age-related hair cell loss and hearing loss in *Sod1^{−/−}* mice that were developed on a 129/CD-1 background (McFadden et al., 1999a; McFadden et al., 1999b). The effects of the *Sod1* gene deletion in these mice, however, were confounded by unknown contributions from segregating *Cdh23* variants and by other strain differences. A subsequent study of *Sod1^{−/−}* mice on a uniform B6 strain background (congenic strain B6.129S7-*Sod1^{tm1Leb}*/DnJ) showed that the absence of SOD1 resulted in hearing loss at an earlier age than in wild-type mice (Keithley et al., 2005). Neither source of *Sod1^{−/−}* mice analyzed in these previous studies, however, allowed for the assessment of the effects of *Sod1^{−/−}* without the confounding effects of *Cdh23^{ahl/ahl}*.

Here we report our efforts to test for the effects of *Sod1* deficiency independently from those of the *Cdh23^{ahl}* hearing loss susceptibility allele by producing and analyzing mice with four digenic genotypes: *Sod1$^{+/+}$Cdh23$^{ahl/ahl}$*, *Sod1$^{+/+}$ Cdh23$^{+/+}$*, *Sod1$^{-/-}$ Cdh23$^{ahl/ahl}$*, and *Sod1$^{-/-}$ Cdh23$^{+/+}$*, all on a uniform B6 strain background. We assessed hearing loss by ABR threshold analysis and evaluated cochlear pathologies in age-matched mice of each of the four digenic combinations. Our findings provide new insights into the specific roles played by tip link integrity (deduced from *Cdh23* genotypic effects) and superoxide radicals (deduced from *Sod1* genotypic effects) in age-related hearing loss and cochlear pathology.

2. Materials and methods

2.1 Mice

All mice examined in this study originated from The Jackson Laboratory (http://www.jax.org/). To generate C57BL/6J (B6) mice with the four experimental *Cdh23 Sod1* digenic genotypes, we first mated B6.CAST-*Cdh23^{Ahl+}*/Kjn strain mice (JAX stock # 2756; genotype *Sod1$^{+/+}$ Cdh23$^{+/+}$*) with B6.129S7-*Sod1^{tm1Leb}*/DnJ strain mice (JAX stock # 3881: genotype *Sod1$^{-/-}$ Cdh23$^{ahl/ahl}$*) to produce F1 hybrids (genotype *Sod1$^{+/-}$ Cdh23$^{+/ahl}$*). The F1 hybrids were then interbred, and F2 intercross progeny with the following four digenic genotypes were selected for study: *Sod1$^{+/+}$ Cdh23$^{+/+}$*, *Sod1$^{+/+}$ Cdh23$^{ahl/ahl}$*, *Sod1$^{-/-}$ Cdh23$^{+/+}$*, and *Sod1$^{-/-}$ Cdh23$^{ahl/ahl}$*.

Experimental mice were housed in the Research Animal Facility of The Jackson Laboratory, and procedures involving their use were approved by the Institutional Animal Care and Use Committee. The Jackson Laboratory is accredited by the American Association for the Accreditation of Laboratory Animal Care.

2.2 Cdh23 and Sod1 genotyping

To genotype F2 mice obtained from the intercross of (B6.CAST-*Cdh23^{Ahl+}*/Kjn X B6.129S7-*Sod1^{tm1Leb}*/DnJ) F1 hybrids, we extracted DNA from tail tips for PCR analysis. To identify *Cdh23* genotypes, we typed individual F2 progeny DNAs for microsatellite markers *D10Mit130* and *D10Mit108*, which flank *Cdh23* and differ in size between C57BL/6J and CAST/EiJ. If both flanking markers were of C57BL/6J origin, the *Cdh23* genotype was presumed to be *ahl/ahl*, and if both flanking markers were of CAST/EiJ origin, the *Cdh23* genotype was presumed to be +/+. For verification, a subsample of mice were genotyped directly by DNA sequence analysis of the *Cdh23^{ahl}* splice site region (Noben-Trauth et al., 2003). The Jackson Laboratory's Transgenic Genotyping Service was used to identify mice with *Sod1$^{+/+}$* and *Sod1$^{-/-}$* genotypes by a quantitative PCR method described online at URL:
http://jaxmice.jax.org/pub-cgi/protocols/protocols.sh?objtype=protocol&protocol_id=2047

2.3 Assessment of hearing

Hearing in mice was assessed by ABR threshold analysis, as previously described (Zheng et al., 1999). Stimulus presentation, ABR acquisition, equipment control and data management were coordinated using computerized equipment from Intelligent Hearing Systems (IHS; Miami, Florida). Briefly, the evoked brainstem responses of anesthetized mice were amplified and averaged and their wave patterns displayed on a computer screen. Broad-band clicks and 8, 16, and 32 kHz tone-bursts were respectively channeled through high frequency transducers into the animals' ear canals. Auditory thresholds were obtained for each specific auditory stimulus by varying the sound pressure level (SPL) to identify the lowest level at which an ABR pattern could be recognized; 100 dB was the maximum SPL presented for all stimuli. With our testing system, average ABR thresholds (in dB SPL) for

normal hearing mice are about 40 dB for click, 30 dB for 8 kHz, 20 dB for 16 kHz, and 45 dB for 32 kHz stimuli.

2.4 Cochlear histology

Cochleas were prepared and evaluated as previously described (Ding et al., 2001; Zheng et al., 2009). Mice were euthanized with CO_2, decapitated, and their bullae quickly removed and opened to expose the inner ear. A small hole was carefully made in the round window through which 10% formalin fixative was gently perfused. The cochlea was then immersed in fixative and shipped to the University of Buffalo for analysis. Cochleas were stained with Ehrlich's hematoxylin solution, the organ of Corti carefully microdissected out into two or three segments and mounted as a flat surface preparation in glycerin on glass slides. Surface preparations were examined with a light microscope (Zeiss Standard, 400X magnification). Inner hair cells (IHC) and outer hair cells (OHC) were counted along successive 0.12–0.24 mm intervals of the organ of Corti beginning at the apex. Hair cells were counted as present if the cell body and cuticular plate were intact. Cochleograms showing percent hair cells missing as a function of percent total distance from the apex were constructed for each animal. Percent hair cell losses were based on laboratory norms for young CBA/CaJ mice (Ding et al., 2001).

2.5 Vestibular histology

Our procedures for assessing the vestibular sensory epithelium have been described previously (Ding et al., 2001; Zheng et al., 2009). The horizontal, superior, and posterior portions of the vestibular cavities were opened by carefully removing the overlying bone. The saccule and utricle were separated from surrounding tissue and the otoconia of the saccule and utricle were removed to visualize the maculae. The ampullae were separated from each semicircular canal by sectioning the nerve fibers, blood vessels and connective tissue and the tissue containing cristae was removed. Specimens were stained with hematoxylin or toluidine blue and mounted in glycerin on glass slides. The surface preparations of each sensory epithelium were viewed with a light microscope (Axioskop, Carl Zeiss) at a magnification of 1000X as described in our earlier publications (Ding et al., 2001; Zheng et al., 2009). The numbers of canal ampullae and the numbers of maculae (either utricle or saccule) examined from each genotype, respectively, were: $Sod1^{+/+}$ $Cdh23^{+/+}$ (n = 6 and 2); $Sod1^{+/+}$ $Cdh23^{ahl/ahl}$ (n = 6 and 4); $Sod1^{-/-}$ $Cdh23^{+/+}$ (n = 4 and 4) and $Sod1^{-/-}$ $Cdh23^{ahl/ahl}$ (n = 6 and 2). Specimens were photographed with a digital camera (SPOT Insight, Diagnostic Instruments Inc), processed with imaging software (SPOT Software, version 4.6) and images assembled with Adobe Photoshop 5.5.

2.6 Statistical analyses

We used the JMP 7.0 interactive statistics and graphics software program (www.JMP.com) to analyze our data and display the results. Statistical significance of the differences between means was determined with the Tukey test, which corrects for multiple pair-wise comparisons. Analysis of variance (ANOVA) F-test statistics were used to determine the significance of the individual effects of *Sod1* and *Cdh23* genotypes and their interaction effects on ABR thresholds and percent hair cell loss.

3. Results

3.1 Age-related hearing loss

ABR thresholds were measured in all four genotypes at 6, 9, 12, and 15 months of age using clicks, and 8, 16, and 32 kHz tone bursts. Table 1 lists the mean ABR thresholds and their variance estimates (standard deviations) for each of the test groups for each test age and

auditory stimulus and the numbers of mice tested in each group. The mean ABR thresholds over time among the four experimental groups (*Cdh23 Sod1* digenic genotypes) are graphically illustrated in Figure 1 for each frequency. Mice with $Sod1^{+/+} Cdh23^{+/+}$ genotypes retained normal ABR thresholds up to 15 months of age. The ABR thresholds of mice with $Sod1^{+/+} Cdh23^{ahl/ahl}$ genotypes remained near normal up to 9 months of age, but then increased rapidly at the higher frequencies so that by 15 months of age the 16 and 32 kHz thresholds exceeded those of $Sod1^{-/-} Cdh23^{+/+}$ mice. ABR thresholds for all frequencies were slightly above normal in $Sod1^{-/-} Cdh23^{+/+}$ mice at 6–9 months of age with moderate increases at 12 and 15 months of age. Mice with both gene mutations, genotype $Sod1^{-/-} Cdh23^{ahl/ahl}$, exhibited the earliest onset and most severe hearing loss of the four groups. ABR thresholds at the higher frequencies appeared greater than predicted for strictly additive effects. For example, at 9 months of age the mean 16 kHz thresholds of singly mutant mice, genotypes $Sod1^{+/+} Cdh23^{ahl/ahl}$ and $Sod1^{-/-} Cdh23^{+/+}$, are similar to each other and only about 10 dB above those of $Sod1^{+/+} Cdh23^{+/+}$ mice, whereas thresholds of doubly mutant $Sod1^{-/-} Cdh23^{ahl/ahl}$ mice are about 60 dB above those of $Sod1^{+/+} Cdh23^{+/+}$ mice. A similar trend was evident at other frequencies and ages.

Detailed comparisons of ABR threshold means and confidence intervals are illustrated in Supplementary Fig. 1. Those genotype pairs with statistically significant mean differences are listed in Table 2 and Supplementary Fig. 1 for each age and test stimulus. At 6 months of age, the *Sod1* genotype had a significant effect on ABR thresholds for all test stimuli, but the *Cdh23* genotype had a significant effect only on 32 kHz thresholds (Table 2). By 9 months of age, however, the individual *Sod1* and *Cdh23* genotypes and their interaction all had significant effects on ABR thresholds, which were seen most strongly at the higher 16 and 32 kHz test frequencies.

3.2 Cochlear pathology

We prepared cytocochleograms from a total of 54 mice having all four experimental genotypes. The mice ranged in age from 6 to 15 months for $Sod1^{-/-} Cdh23^{+/+}$ and $Sod1^{-/-} Cdh23^{ahl/ahl}$, 9 to 15 months for $Sod1^{+/+} Cdh23^{ahl/ahl}$, and 12 to 15 months for $Sod1^{+/+} Cdh23^{+/+}$. Figure 2 shows the total percent OHC loss and the percent IHC loss along the entire length of the cochlea for each of the four genotypes. Mice with the $Cdh23^{ahl/ahl}$ genotype, regardless of *Sod1* genotype, showed a large increase in both OHC and IHC loss between 6 and 15 months of age. This trend was most pronounced in $Sod1^{-/-} Cdh23^{ahl/ahl}$ mice followed closely by $Sod1^{+/+} Cdh23^{ahl/ahl}$ mice; OHC and IHC lesions in these two strains were prominent at 9 months of age and tended to increase with advancing age. In contrast, mice with the $Cdh23^{+/+}$ genotype, regardless of *Sod1* genotype ($Sod1^{-/-} Cdh23^{+/+}$ and $Sod1^{+/+} Cdh23^{+/+}$ mice), showed only a modest increase in OHC loss, which developed later in life between 12 and 15 month of age. $Sod1^{-/-} Cdh23^{+/+}$ mice showed little IHC loss even at 12–15 months of age, but surprisingly $Sod1^{+/+} Cdh23^{+/+}$ mice showed approximately a 30% IHC loss at 12–15 months of age.

Figure 3 shows the mean IHC and OHC loss as a function of percent distance from the apex in 12-month-old and 15-month-old mice of each digenic genotype. The arrows show the relationship of 8, 16 and 32 kHz test frequencies to the cochlear place map (Muller et al., 2005). Each point represents the percent hair cell loss at 20% intervals along the cochlear duct. At both ages, $Sod1^{-/-} Cdh23^{ahl/ahl}$ mice showed a large OHC and IHC loss, which was greatest near the base of the cochlea (100%) and decreased towards the apex. $Sod1^{+/+} Cdh23^{ahl/ahl}$ mice showed a similar pattern of IHC and OHC loss at both ages; however the degree of damage was slightly less than in $Sod1^{-/-} Cdh23^{ahl/ahl}$ mice in the apical half of the cochlea. In contrast, the $Sod1^{-/-} Cdh23^{+/+}$ mice showed little IHC loss at 12 and 15 months; however, OHC loss in this genotype was atypical being greatest near the apex (30–40%) and declining towards the base. Unexpectedly, $Sod1^{+/+} Cdh23^{+/+}$ mice exhibited 40–

50% IHC loss near the middle of the cochlea at 12 and 15 months whereas OHC loss at 15 months was approximately 35% near the apex and 30% in the base of the cochlea.

Detailed comparisons of means and confidence intervals for estimates of percent IHC and OHC loss in combined 12- and 15-month old mice are illustrated in Supplementary Fig. 2, for hair cell counts along the entire cochlea and for regions 30%, 50%, and 70% from the cochlear apex. Those digenic genotype pairs with statistically significant mean differences are listed in Table 3 and Supplementary Fig. 2. The *Sod1* genotype by itself had a statistically significant effect only on IHC loss 70% from apex region and OHC loss 50% from the apex (Table 3). The *Cdh23* genotype, in contrast, had a large effect on hair cell loss at the base to mid-region of the cochlea, but had little effect on hair cells in regions less than 40% from the apex. The *Sod1*Cdh23* genotype interaction had no significant effect on OHC loss in any cochlear region; however a significant interaction occurred for IHC loss 50% and 70% from the cochlear apex.

3.3 Vestibular Hair Cells

The protein encoded by *Cdh23* is not only expressed in the cochlea, but is also expressed in the stereocilia of vestibular hair cells (Lagziel et al., 2005; Wilson et al., 2001). Since there was considerable age-related degeneration of cochlear hair cells in $Cdh23^{ahl/ahl}$ mice, we examined the hair cells in the macula of the saccule and utricle and in the ampulla of the semicircular canals. Figure 4 shows the status of these vestibular hair cells in 12-month-old mice of each digenic genotype. Despite extensive damage to cochlear hair cells, vestibular hair cell densities appeared remarkably normal and similar across the four genotypes, even in mice with both $Sod1^{-/-}$ and $Cdh23^{ahl/ahl}$ deficiencies.

4. Discussion

Hearing loss progression is more rapid at the high frequencies in $Sod1^{+/+}$ $Cdh23^{ahl/ahl}$ and $Sod1^{-/-}$ $Cdh23^{ahl/ahl}$ mice than in $Sod1^{-/-}$ $Cdh23^{+/+}$ mice, which show a less frequency-dependent progression (Fig. 1; Table 1). The increase in hearing loss at high frequencies is consistent with the cochleograms of $Sod1^{+/+}$ $Cdh23^{ahl/ahl}$ and $Sod1^{-/-}$ $Cdh23^{ahl/ahl}$ mice, which show the greatest IHC and OHC loss at the basal region of the cochlear duct (Fig. 3). The proposed role of CDH23 as a component of stereocilia tip links offers a potential explanation for these results (Schwander et al., 2009). Hair cells near the cochlear base have greater numbers of stereocilia than more apical hair cells, and OHCs have greater numbers of stereocilia than IHCs (Lim, 1986). Because OHCs near the base of the cochlea have the greatest number of stereocilia, they also have the greatest number of tip links and thus may be the most vulnerable to damage conferred by the detrimental *ahl* allelic form of CDH23. Because vestibular hair cells are subjected to much lower frequency stimulations than cochlear hair cells, tip links may be less detrimental, and this mechanism could explain why $Cdh23^{ahl/ahl}$ mice with profound hearing loss maintain normal balance function and lack vestibular hair cell damage (Fig. 4).

It is possible that the tip link abnormalities related to $Cdh23^{ahl}$ may cause an increase in the open probability of the mechanoelectrical transduction (MET) channel, and consequent leakage of cations may lead to a frequent state of depolarization, especially in hair cells with large numbers of stereocilia and MET channels (such as basal OHCs). This depolarization would open calcium channels in the basolateral membrane causing excessive entry of Ca^{2+} that might then lead to hair cell death. In support of this possible mechanism, $Cdh23^{ahl}$ has been shown to greatly exacerbate the effects of the deaf waddler (*dfw*) mutation of the *Atp2b2* gene (Noben-Trauth et al., 2003), which encodes the PMCA2 calcium pump of hair cell stereocilia. A similar mechanism of Ca^{2+}-related hair cell pathology has been proposed for the *dfw* mutation, in which defective PMCA2 decreases the Ca^{2+} concentration in the

endolymph surrounding stereocilia tips and thereby causes a reduction in adaptation and an increase in the open probability of MET channels (Ficarella et al., 2007). Chronic depolarization causing Ca^{2+} influx through voltage-gated Ca^{2+} channels is also thought to underlie the selective degeneration of high frequency OHCs and progressive hearing loss in mice lacking KCNQ4-mediated K^+ currents (Kharkovets et al., 2006). Calcium dysregulation also has been implicated in noise-induced hearing loss, NIHL (Fridberger et al., 1998; Shen et al., 2007), and calcium overload associated with NIHL has been shown to activate mitochondria-mediated cell death pathways in outer hair cells (Vicente-Torres et al., 2006).

Another explanation for the base-apex gradient of hair cell dysfunction is that hair cells in the base of the cochlea are more vulnerable to oxidative stress because the glutathione antioxidant enzyme is lower in the base of the cochlea than the apex (Sha et al., 2001). Thus, defects in CDH23 combined with reduced expression of glutathione would impose greater oxidative stress on hair cells in the base versus apex resulting in early onset, high-frequency hearing loss, consistent with our ABR data. Glutathione immunolabeling is slightly higher in vestibular hair cells than cochlear hair cells which may explain why vestibular hair cells are resistant to the *ahl* allelic form of CDH23 (Usami et al., 1996).

The degree of high frequency hearing loss in mice with both *Sod1* and *Cdh23* deficits is much greater than expected from additive effects of each gene (Fig. 1, Table 2) and indicates some type of synergistic interaction. Hair cells of $Cdh23^{ahl/ahl}$ mice are likely to become stressed from frequent tip link breakage and repair or calcium influx, and this increased stress would increase energy demands on mitochondria leading to an accumulation of ROS. A similar mechanism of ROS formation has been proposed for noise-induced hearing loss, which also includes broken tip links among the physical changes it induces (Henderson et al., 2006). A study of the expression levels of antioxidant enzymes in aging mouse cochleas showed much higher increases in B6 mice compared with B6.CAST-$Cdh23^{Ahl+}$ congenic mice, which suggests that the $Cdh23^{ahl}$ variant may be associated with an increase in oxidative stress (Staecker et al., 2001). Calcium toxicity or increased levels of ROS caused by $Cdh23^{ahl/ahl}$ when combined with a decrease in antioxidant defense caused by $Sod1^{-/-}$ could have a severe effect on hair cell metabolism and viability in $Sod1^{-/-} Cdh23^{ahl/ahl}$ mice resulting in a rapid progression of hearing loss (Fig. 1) and an increased loss of hair cells (Fig. 2).

OHC and IHC losses in $Sod1^{+/+} Chd23^{ahl/ahl}$ and $Sod1^{-/-} Cdh23^{ahl/ahl}$ mice spread from the base to the apex with advancing age, but hair cell loss in the apical 40% of the cochlea was less severe in $Sod1^{+/+} Cdh23^{ahl/ahl}$ mice (Fig. 3C,G) than in $Sod1^{-/-} Cdh23^{ahl/ahl}$ mice (Fig. 3G,H). The hearing loss at 32 kHz was severe in $Sod1^{+/+} Cdh23^{ahl/ahl}$ mice, presumably due to the complete loss of OHCs in the region (Fig. 3C,G). The 32 kHz losses, however, developed more slowly and tended to be less severe in these mice than in $Sod1^{-/-} Cdh23^{ahl/ahl}$ mice (Fig. 1), presumably because acoustic energy from 32 kHz tone bursts was spilling over into the 8–16 kHz cochlear regions where there is less OHC loss (compare Figure 3G with 3H). A more accurate assessment of the threshold near the border of the hearing loss may require the use of notch noise or other masking paradigms as previously noted (Purdy et al., 2002). Since mouse ABR thresholds are normally lowest in the 16 kHz region, downward spectral splatter likely leads to an underestimate of 32 kHz ABR thresholds. Hearing loss in $Sod1^{+/+} Chd23^{ahl/ahl}$ mice is moderate at 16 kHz, which maps to the apical edge of the OHC lesion; again downward spectral splatter likely leads to an underestimate of 16 kHz thresholds in these mice. Hearing loss is minimal at 8 kHz where OHC loss was around 30%.

Hair cell losses in $Sod1^{-/-}$ $Cdh23^{+/+}$ mice were minimal at 12 months of age, but at 15 months a peculiar, reverse apex-to-base gradient of OHC loss appeared. OHC losses were roughly 40%, 30%, and 20% in the 8, 16, and 32 kHz regions of the cochlea, respectively (Figure 3F). Between 9 and 15 months of age, ABR thresholds at 8, 16 and 32 kHz increased by 28, 27 and 24 dB, respectively (Table 1). In addition to the moderate OHC loss, other possible explanations for the ABR threshold shifts in $Sod1^{-/-}$ $Cdh23^{+/+}$ mice include subtle hair cell pathologies that are not reflected in the cochleogram or damage to the fibrocytes in the spiral ligament (Hequembourg et al., 2001).

In $Sod1^{+/+}$ $Cdh23^{+/+}$ mice at 15 months of age, OHC losses in cochlear regions associated with 8, 16 and 32 kHz were roughly 35%, 20% and 10% respectively, and corresponding ABR thresholds increased less than 10 dB between 6 and 15 months of age. Surprisingly, IHC losses in cochlear regions associated with 16 and 32 kHz were quite large, on the order of 45–50%. Why were ABR thresholds unaffected by the IHC lesions? Previous studies have noted that auditory nerve fiber thresholds are essentially normal in animals with selective loss of IHC and type-I spiral ganglion neurons; however, neural thresholds increase significantly with selective OHC lesion (Dallos et al., 1978; Wang et al., 1997). Selective destruction of 30% of the IHC also has little effect on the compound action potential thresholds, although it reduces the amplitude of the compound action potential by approximately 30% (Qiu et al., 2000; Trautwein et al., 1996). The IHC loss in the middle of the cochlea was not observed in $Sod1^{-/-}$ $Cdh23^{+/+}$ mice (Figure 3B, F), and we are at a loss to explain this unusual IHC lesion in the $Sod1^{+/+}$ $Cdh23^{+/+}$ mice other than the possibility of unknown environmental factors or genetic interactions.

Hair cell loss in the basal half of the cochlea was strongly associated with $Cdh23$ genotypes, but was little affected by $Sod1$ genotypes (Figure 3, Table 3). In contrast, ABR thresholds at 16 and 32 kHz frequencies, which map to the basal half of the cochlea, are influenced by genetic deficiencies at both loci. These results imply that $Sod1$ deficiency by itself impairs cochlear function without triggering hair cell apoptosis. Perhaps in the absence of the cellular stress caused by tip link breakage associated with the $Cdh23^{ahl/ahl}$ genotype, a moderate increase in the level of ROS caused by SOD1 deficiency in hair cells of $Sod1^{-/-}$ $Cdh23^{+/+}$ mice may be enough to impair the physiological function of hair cells (or other cochlear structures) but not severe enough to activate signal transduction pathways initiating hair cell death. A recent study has provided evidence that OHC dysfunction, as indicated by perturbed mitochondrial metabolism, can occur well before cellular death in organ of Corti cultures subjected to oxidative stress induced by aminoglycoside exposure (Tiede et al., 2009). Non-lethal impairment of OHC function has also been proposed to explain some of the hearing loss exhibited by aged rats (Chen et al., 2009).

The $Cdh23^{ahl/ahl}$ (Davis et al., 2001) and $Sod^{-/-}$ (Ohlemiller et al., 1999) genotypes have been shown to increase the susceptibility of mice to noise-induced hearing loss (NIHL) as well as to AHL. That AHL and NIHL share these same genetic susceptibility factors suggests that aging and noise trauma may promote common cochlear injuries (Ohlemiller, 2006). It will be interesting to see if the specific $Cdh23^{ahl/ahl}$ and $Sod^{-/-}$ genotype combinations we report here for AHL have similar effects on NIHL and its associated cochlear pathologies.

In summary, we have taken a genetic approach to analyze individual and combined effects of $Cdh23^{ahl}$ and $Sod1^{-}$ mutations on age-related hearing loss and cochlear pathology in C57BL/6J mice. We show that mice homozygous for either gene mutation exhibit progressive hearing loss compared with non-mutant controls, but that hearing loss in $Cdh23^{ahl/ahl}$ mice is greater at high frequencies, while that of $Sod^{-/-}$ mice is less frequency-dependent. Mice homozygous for both mutations exhibit an accelerated high frequency

hearing loss, which is greater than expected from solely additive effects. Mice homozygous for the *Cdh23^{ahl}* mutation, whether alone or in combination with *Sod1⁻*, exhibit a progressive base to apex loss of cochlear hair cells but no loss of vestibular hair cells. Mice homozygous for the *Sod1⁻* mutation but without the *Cdh23^{ahl}* mutation show little if any loss of cochlear hair cells, in contrast to their elevated ABR thresholds. Possible mechanisms that may underlie these results are discussed in the context of previously proposed effects of *Cdh23^{ahl}* on stereocilia tip link integrity and *Sod1⁻* on cochlear vulnerability to ROS damage.

Supplementary Material

Refer to Web version on PubMed Central for supplementary material.

Acknowledgments

Abbreviations

ABR	auditory brainstem response
AHL	age-related hearing loss
NIHL	noise-induced hearing loss
IHC	inner hair cell
OHC	outer hair cell
st dev	standard deviation

References

Chen GD, Li M, Tanaka C, Bielefeld EC, Hu BH, Kermany MH, Salvi R, Henderson D. Aging outer hair cells (OHCs) in the Fischer 344 rat cochlea: function and morphology. Hear Res 2009;248:39–47. [PubMed: 19111601]

Dallos P, Harris D. Properties of auditory nerve responses in absence of outer hair cells. J Neurophysiol 1978;41:365–83. [PubMed: 650272]

Dalton DS, Cruickshanks KJ, Klein BE, Klein R, Wiley TL, Nondahl DM. The impact of hearing loss on quality of life in older adults. Gerontologist 2003;43:661–8. [PubMed: 14570962]

Davis RR, Newlander JK, Ling X, Cortopassi GA, Krieg EF, Erway LC. Genetic basis for susceptibility to noise-induced hearing loss in mice. Hear Res 2001;155:82–90. [PubMed: 11335078]

DeStefano AL, Gates GA, Heard-Costa N, Myers RH, Baldwin CT. Genomewide linkage analysis to presbycusis in the Framingham Heart Study. Arch Otolaryngol Head Neck Surg 2003;129:285–9. [PubMed: 12622536]

Ding, D.; McFadden, SL.; Salvi, R. Cochlear Hair Cell Densities and Inner-Ear Staining Techniques. In: Willott, JF., editor. Handbook of Mouse auditory Research from Behavior to Molecular Biology. CRC Press; Boca Raton: 2001. p. 189-204.

Ficarella R, Di Leva F, Bortolozzi M, Ortolano S, Donaudy F, Petrillo M, Melchionda S, Lelli A, Domi T, Fedrizzi L, Lim D, Shull GE, Gasparini P, Brini M, Mammano F, Carafoli E. A functional study of plasma-membrane calcium-pump isoform 2 mutants causing digenic deafness. Proc Natl Acad Sci U S A 2007;104:1516–21. [PubMed: 17234811]

Fridberger A, Flock A, Ulfendahl M, Flock B. Acoustic overstimulation increases outer hair cell Ca2+ concentrations and causes dynamic contractions of the hearing organ. Proc Natl Acad Sci U S A 1998;95:7127–32. [PubMed: 9618550]

Friedman RA, Van Laer L, Huentelman MJ, Sheth SS, Van Eyken E, Corneveaux JJ, Tembe WD, Halperin RF, Thorburn AQ, Thys S, Bonneux S, Fransen E, Huyghe J, Pyykko I, Cremers CW, Kremer H, Dhooge I, Stephens D, Orzan E, Pfister M, Bille M, Parving A, Sorri M, Van de Heyning PH, Makmura L, Ohmen JD, Linthicum FH Jr, Fayad JN, Pearson JV, Craig DW, Stephan DA, Van Camp G. GRM7 variants confer susceptibility to age-related hearing impairment. Hum Mol Genet 2009;18:785–796. [PubMed: 19047183]

Henderson D, Bielefeld EC, Harris KC, Hu BH. The role of oxidative stress in noise-induced hearing loss. Ear Hear 2006;27:1–19. [PubMed: 16446561]

Henry KR, Chole RA. Genotypic differences in behavioral, physiological and anatomical expressions of age-related hearing loss on the laboratory mouse. Audiology 1980;19:369–383. [PubMed: 7436856]

Hequembourg S, Liberman MC. Spiral ligament pathology: a major aspect of age-related cochlear degeneration in C57BL/6 mice. J Assoc Res Otolaryngol 2001;2:118–29. [PubMed: 11550522]

Jiang H, Talaska AE, Schacht J, Sha SH. Oxidative imbalance in the aging inner ear. Neurobiol Aging 2007;28:1605–12. [PubMed: 16920227]

Johnson KR, Zheng QY, Erway LC. A major gene affecting age-related hearing loss is common to at least ten inbred strains of mice. Genomics 2000;70:171–180. [PubMed: 11112345]

Johnson KR, Erway LC, Cook SA, Willott JF, Zheng QY. A major gene affecting age-related hearing loss in C57BL/6J mice. Hear Res 1997;114:83–92. [PubMed: 9447922]

Kazmierczak P, Sakaguchi H, Tokita J, Wilson-Kubalek EM, Milligan RA, Muller U, Kachar B. Cadherin 23 and protocadherin 15 interact to form tip-link filaments in sensory hair cells. Nature 2007;449:87–91. [PubMed: 17805295]

Keithley EM, Canto C, Zheng QY, Fischel-Ghodsian N, Johnson KR. Age-related hearing loss and the ahl locus in mice. Hear Res 2004;188:21–8. [PubMed: 14759567]

Keithley EM, Canto C, Zheng QY, Wang X, Fischel-Ghodsian N, Johnson KR. Cu/Zn superoxide dismutase and age-related hearing loss. Hear Res 2005;209:76–85. [PubMed: 16055286]

Kharkovets T, Dedek K, Maier H, Schweizer M, Khimich D, Nouvian R, Vardanyan V, Leuwer R, Moser T, Jentsch TJ. Mice with altered KCNQ4 K(+) channels implicate sensory outer hair cells in human progressive deafness. EMBO J 2006;25:642–652. [PubMed: 16437162]

Lagziel A, Ahmed ZM, Schultz JM, Morell RJ, Belyantseva IA, Friedman TB. Spatiotemporal pattern and isoforms of cadherin 23 in wild type and waltzer mice during inner ear hair cell development. Dev Biol 2005;280:295–306. [PubMed: 15882574]

Lim DJ. Functional structure of the organ of Corti: a review. Hear Res 1986;22:117–146. [PubMed: 3525482]

McFadden SL, Ding D, Salvi R. Anatomical, metabolic and genetic aspects of age-related hearing loss in mice. Audiology 2001;40:313–21. [PubMed: 11781044]

McFadden SL, Ding D, Reaume AG, Flood DG, Salvi RJ. Age-related cochlear hair cell loss is enhanced in mice lacking copper/zinc superoxide dismutase. Neurobiol Aging 1999a;20:1–8. [PubMed: 10466888]

McFadden SL, Ding D, Burkard RF, Jiang H, Reaume AG, Flood DG, Salvi RJ. Cu/Zn SOD deficiency potentiates hearing loss and cochlear pathology in aged 129,CD-1 mice. J Comp Neurol 1999b;413:101–12. [PubMed: 10464373]

Mikaelian DO. Development and degeneration of hearing in the C57/bl6 mouse: relation of electrophysiologic responses from the round window and cochlear nucleus to cochlear anatomy and behavioral responses. Laryngoscopy 1979;34:1–15.

Muller M, von Hunerbein K, Hoidis S, Smolders JW. A physiological place-frequency map of the cochlea in the CBA/J mouse. Hear Res 2005;202:63–73. [PubMed: 15811700]

Noben-Trauth K, Zheng QY, Johnson KR. Association of cadherin 23 with polygenic inheritance and genetic modification of sensorineural hearing loss. Nat Genet 2003;35:21–23. [PubMed: 12910270]

Ohlemiller KK. Contributions of mouse models to understanding of age- and noise-related hearing loss. Brain Res 2006;1091:89–102. [PubMed: 16631134]

Ohlemiller KK, McFadden SL, Ding DL, Flood DG, Reaume AG, Hoffman EK, Scott RW, Wright JS, Putcha GV, Salvi RJ. Targeted deletion of the cytosolic Cu/Zn-superoxide dismutase gene (Sod1) increases susceptibility to noise-induced hearing loss. Audiol Neurootol 1999;4:237–46. [PubMed: 10436316]

Purdy SC, Abbas PJ. ABR thresholds to tonebursts gated with Blackman and linear windows in adults with high-frequency sensorineural hearing loss. Ear Hear 2002;23:358–68. [PubMed: 12195178]

Qiu C, Salvi R, Ding D, Burkard R. Inner hair cell loss leads to enhanced response amplitudes in auditory cortex of unanesthetized chinchillas: evidence for increased system gain. Hear Res 2000;139:153–71. [PubMed: 10601720]

Schwander M, Xiong W, Tokita J, Lelli A, Elledge HM, Kazmierczak P, Sczaniecka A, Kolatkar A, Wiltshire T, Kuhn P, Holt JR, Kachar B, Tarantino L, Muller U. A mouse model for nonsyndromic deafness (DFNB12) links hearing loss to defects in tip links of mechanosensory hair cells. Proc Natl Acad Sci U S A 2009;106:5252–7. [PubMed: 19270079]

Sha SH, Taylor R, Forge A, Schacht J. Differential vulnerability of basal and apical hair cells is based on intrinsic susceptibility to free radicals. Hear Res 2001;155:1–8. [PubMed: 11335071]

Shen H, Zhang B, Shin J-H, Lei D, Du Y, Gao X, Wang Q, Ohlemiller KK, Piccirillo J, Bao J. Prophylactic and therapeutic functions of T-type calcium blockers against noise-induced hearing loss. Hear Res 2007;226:52–60. [PubMed: 17291698]

Spongr VP, Flood DG, Frisina RD, Salvi RJ. Quantitative measures of hair cell loss in CBA and C57BL/6 mice throughout their life spans. J Acoust Soc Am 1997;101:3546–53. [PubMed: 9193043]

Staecker H, Zheng QY, Van De Water TR. Oxidative stress in aging in the C57B16/J mouse cochlea. Acta Otolaryngol 2001;121:666–72. [PubMed: 11678164]

Tiede L, Steyger PS, Nichols MG, Hallworth R. Metabolic imaging of the organ of corti--a window on cochlea bioenergetics. Brain Res 2009;1277:37–41. [PubMed: 19272358]

Trautwein P, Hofstetter P, Wang J, Salvi R, Nostrant A. Selective inner hair cell loss does not alter distortion product otoacoustic emissions. Hear Res 1996;96:71–82. [PubMed: 8817308]

Usami S, Hjelle OP, Ottersen OP. Differential cellular distribution of glutathione--an endogenous antioxidant--in the guinea pig inner ear. Brain Res 1996;743:337–40. [PubMed: 9017265]

Vicente-Torres MA, Schacht J. A BAD link to mitochondrial cell death in the cochlea of mice with noise-induced hearing loss. J Neurosci Res 2006;83:1564–1572. [PubMed: 16521126]

Wang J, Powers NL, Hofstetter P, Trautwein P, Ding D, Salvi R. Effects of selective inner hair cell loss on auditory nerve fiber threshold, tuning and spontaneous and driven discharge rate. Hear Res 1997;107:67–82. [PubMed: 9165348]

Wang J, Menchenton T, Yin S, Yu Z, Bance M, Morris DP, Moore CS, Korneluk RG, Robertson GS. Over-expression of X-linked inhibitor of apoptosis protein slows presbycusis in C57BL/6J mice. Neurobiol Aging. 2008

Willott JF. Effects of aging, hearing loss and anatomical location on thresholds of inferior colliculus neurons in C57BL/6 and CBA mice. J Neurophysiol 1986;56:391–408. [PubMed: 3760927]

Wilson SM, Householder DB, Coppola V, Tessarollo L, Fritzsch B, Lee EC, Goss D, Carlson GA, Copeland NG, Jenkins NA. Mutations in Cdh23 cause nonsyndromic hearing loss in waltzer mice. Genomics 2001;74:228–33. [PubMed: 11386759]

Zheng QY, Johnson KR, Erway LC. Assessment of hearing in 80 inbred strains of mice by ABR threshold analyses. Hear Res 1999;130:94–107. [PubMed: 10320101]

Zheng QY, Ding D, Yu H, Salvi RJ, Johnson KR. A locus on distal chromosome 10 (ahl4) affecting age-related hearing loss in A/J mice. Neurobiol Aging 2009;30:1693–1705. [PubMed: 18280008]
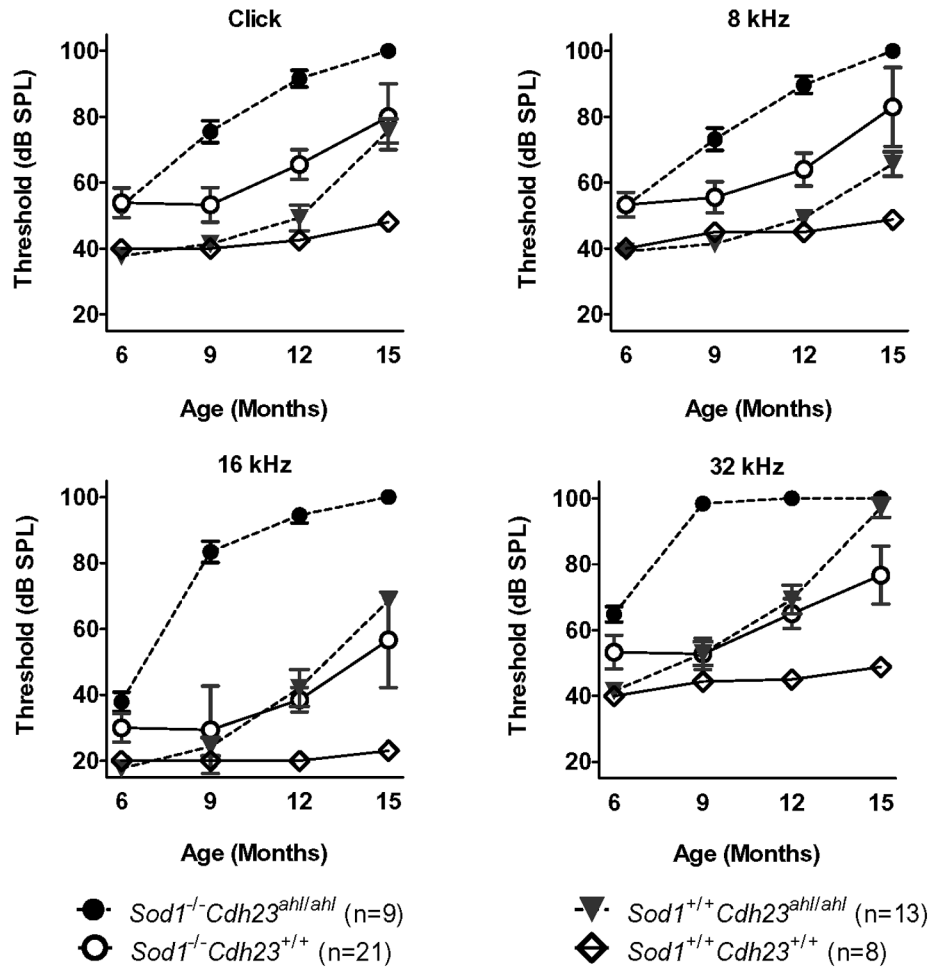
Figure 1. Effects of genotype, age and auditory stimulus on ABR thresholds
ABR thresholds (means ± standard errors) are compared among mice with four different digenic genotypes of *Cdh23* and *Sod1*, all on a uniform C57BL/6J background. Mice were tested at 6, 9, 12, and 15 months of age, and ABRs were recorded for broad-band click and 8 kHz, 16 kHz, and 32 kHz pure tone stimuli. The numbers of mice evaluated for each genotype and test age are given in Table 1.
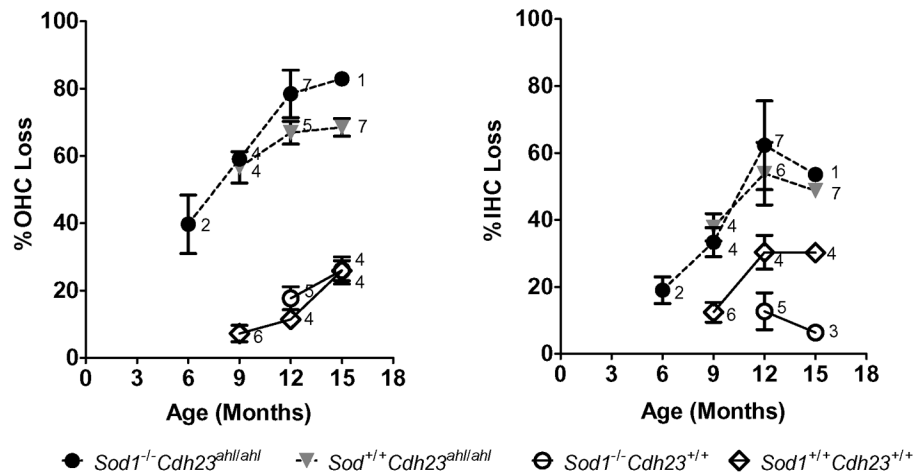
Figure 2. Effects of genotype and age on cochlear hair cell loss
Mean percentage (± standard error) loss of OHC and IHC along the entire length of the cochlea is shown as a function of age for four different digenic genotypes of *Cdh23* and *Sod1*, all on a uniform C57BL/6J genetic background. Numbers next to each symbol indicate sample size.
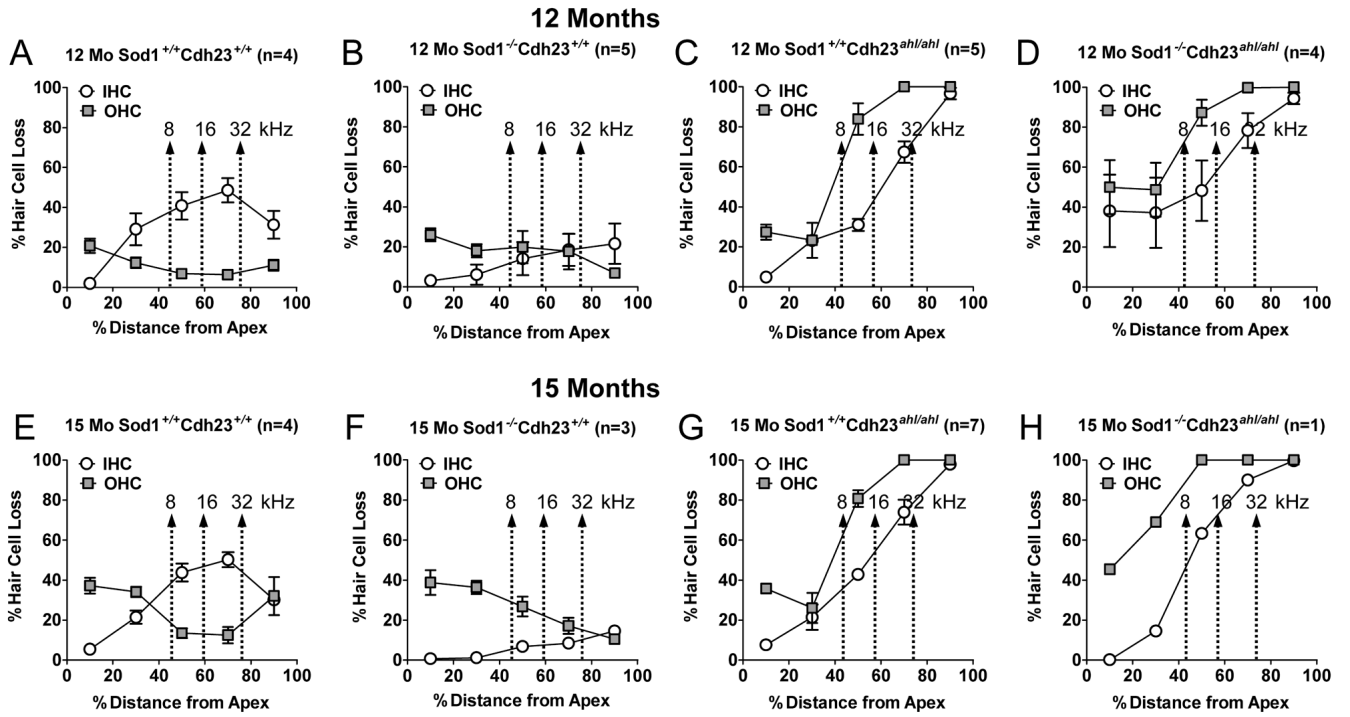
12 Months

15 Months

Figure 3. Effects of genotype and cochlear location on hair cell loss
Cochleograms show the means ± standard errors of the percent IHC and OHC loss in 12 and 15 month old mice for each of the four digenic genotypes of *Cdh23* and *Sod1*, all on a uniform C57BL/6J genetic background. Each point represents the percent hair cell loss in 20% intervals along the cochlear duct. The arrows show the positions along the cochlear place map that correspond to the 8, 16 and 32 kHz test frequencies (Muller et al., 2005).
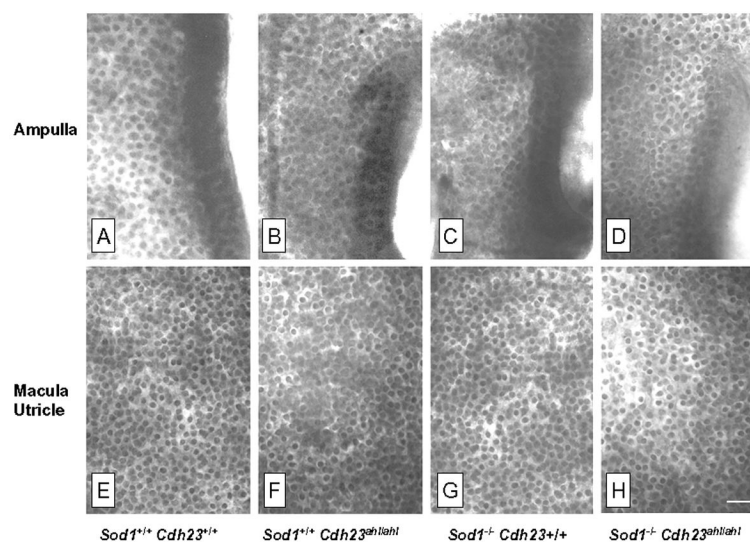
Ampulla

A   B   C   D

**Macula
Utricle**

E   F   G   H

Sod1⁺/⁺ Cdh23⁺/⁺   *Sod1⁺/⁺ Cdh23ᵃʰˡ/ᵃʰˡ*   *Sod1⁻/⁻ Cdh23+/+*   *Sod1⁻/⁻ Cdh23ᵃʰˡ/ᵃʰˡ*

Figure 4. Histology of vestibular hair cells
Representative photomicrographs showing the density of vestibular hair cells in the ampulla (top row, A-D) and macula of the utricle (bottom row, E-H) in 12-month-old mice with the four different digenic genotypes of *Cdh23* and *Sod1*. All panel images are shown at the same magnification. Scale bar 30 μm, shown in Panel H.

Table 1

Means and standard deviations (st dev) of ABR thresholds (dB SPL) for each genotype, test age, and auditory stimulus

		genotype "A" *Sod1+/+Cdh23+/+*	genotype "B" *Sod1+/+Cdh23ahl/ahl*	genotype "C" *Sod1−/−Cdh23+/+*	genotype "D" *Sod1−/−Cdh23ahl/ahl*
6 month test age		N = 8	N = 13	N = 9	N = 21
click	mean	**39.4**	**37.7**	**53.9**	**52.9**
	st dev	1.8	3.9	13.6	8.5
8 kHz	mean	**40.0**	**39.2**	**53.3**	**52.9**
	st dev	0.0	1.9	11..2	8.5
16 kHz	mean	**20.0**	**17.7**	**30.0**	**37.9**
	st dev	0.0	3.3	13.0	13.1
32 kHz	mean	**40.0**	**41.5**	**53.3**	**64.8**
	st dev	0.0	3.2	15.2	11.2
9 month test age		N = 8	N = 7	N = 9	N = 22
click	mean	**40.0**	**41.4**	**53.3**	**75.5**
	st dev	0.0	3.8	15.8	15.6
8 kHz	mean	**45.0**	**41.4**	**55.6**	**73.2**
	st dev	5.3	3.8	14.2	15.9
16 kHz	mean	**20.0**	**24.3**	**29.4**	**83.4**
	st dev	0.0	7.3	13.3	15.1
32 kHz	mean	**44.4**	**52.9**	**52.8**	**98.4**
	st dev	5.0	9.5	14.4	5.6
12 month test age		N = 8	N = 7	N = 10	N = 17
click	mean	**42.5**	**49.3**	**65.5**	**91.6**
	st dev	4.8	10.2	14.2	10.8
8 kHz	mean	**45.0**	**49.3**	**64.0**	**89.7**
	st dev	5.3	6.1	15.8	10.9
16 kHz	mean	**20.0**	**42.1**	**38.5**	**94.5**
	st dev	0.0	14.7	11.6	9.6
32 kHz	mean	**45.0**	**69.3**	**65.0**	**100**
	st dev	5.3	11.7	14.3	0.0

		genotype "A" $Sod1^{+/+}Cdh23^{+/+}$	genotype "B" $Sod1^{+/+}Cdh23^{ahl/ahl}$	genotype "C" $Sod1^{-/-}Cdh23^{+/+}$	genotype "D" $Sod1^{-/-}Cdh23^{ahl/ahl}$
15 month test age		N = 8	N = 7	N = 3	N = 2
click	mean	48.1	75.7	80.0	100
	st dev	3.7	9.8	17.3	0.0
8 kHz	mean	48.8	65.7	83.3	100
	st dev	3.5	9.8	20.8	0.0
16 kHz	mean	23.1	68.6	56.7	100
	st dev	5.3	3.8	25.2	0.0
32 kHz	mean	48.8	97.1	76.7	100
	st dev	3.5	7.6	15.3	0.0

Table 2
Statistical analyses of ABR thresholds

Analysis of variance (ANOVA) F-tests were used to evaluate the separate and interactive effects of *Sod1* and *Cdh23* genotypes on click, 8 kHz, 16 kHz, and 32 kHz thresholds of mice tested at 6, 9, 12, and 15 months of age. The probabilities of obtaining the calculated F ratios solely by chance are shown for each effect in each stimulus-age category. Statistically significant effects at the 0.05 alpha level are indicated by a single asterisk and at the 0.001 level by two asterisks. The digenic genotypes for the Tukey pair-wise tests of means are indicated by letters as follows: *Sod1$^{+/+}$ Cdh23$^{+/+}$* (**A**), *Sod1$^{+/+}$ Cdh23$^{ahl/ahl}$* (**B**), *Sod1$^{-/-}$ Cdh23$^{+/+}$* (**C**), *Sod1$^{-/-}$ Cdh23$^{ahl/ahl}$* (**D**). Only those genotype pairs with significant mean differences at the 0.05 alpha level are shown.

	6 mo	9 mo	12 mo	15 mo
Click				
ANOVA for monogenic genotypes				
Sod1 main effect	<0.0001 **	<0.0001 **	<0.0001 **	<0.0001 **
Cdh23 main effect	0.582	0.008 *	<0.0001 **	<0.0001 **
*Sod1*Cdh23* interaction	0.895	0.020 *	0.009 *	0.429
Tukey pair-wise tests of digenic genotypes				
significant mean differences (p<0.05)	A-C, A-D, B-C, B-D	A-D, B-D, C-D	A-C, A-D, B-C, B-D, C-D	A-B, A-C, A-D, B-D
8 kHz				
ANOVA for monogenic genotypes				
Sod1 main effect	<0.0001 **	<0.0001 **	<0.0001 **	<0.0001 **
Cdh23 main effect	0.776	0.107	0.0001 **	0.0047 *
*Sod1*Cdh23* interaction	0.947	0.017 *	0.0043 *	0.977
Tukey pair-wise tests of digenic genotypes				
significant mean differences (p<0.05)	A-C, A-D, B-C, B-D	A-D, B-D, C-D	A-C, A-D, B-C, B-D, C-D	A-B, A-C, A-D, B-D
16 kHz				
ANOVA for monogenic genotypes				
Sod1 main effect	<0.0001 **	<0.0001 **	<0.0001 **	<0.0001 **
Cdh23 main effect	0.371	<0.0001 **	<0.0001 **	<0.0001 **
*Sod1*Cdh23* interaction	0.104	<0.0001 **	<0.0001 **	0.840
Tukey pair-wise tests of digenic genotypes				
significant mean differences (p<0.05)	A-D, B-C, B-D	A-D, B-D, C-D	A-B, A-C, A-D, B-D, C-D	A-B, A-C, A-D, B-D, C-D
32 kHz				
ANOVA for monogenic genotypes				
Sod1 main effect	<0.0001 **	<0.0001 **	<0.0001 **	0.0012 *
Cdh23 main effect	0.032 *	<0.0001 **	<0.0001 **	<0.0001 **
*Sod1*Cdh23* interaction	0.099	<0.0001 **	0.058	0.0057 *
Tukey pair-wise tests of digenic genotypes				
significant mean differences (p<0.05)	A-C, A-D, B-C, B-D, C-D	A-D, B-D, C-D	A-B, A-C, A-D, B-D, C-D	A-B, A-C, A-D, B-C, C-D

Table 3
Statistical analyses of percent hair cell loss

Mice of the 12- and 15-month age groups were combined for these analyses. Analysis of variance (ANOVA) F-tests were used to evaluate the separate and interactive effects of *Sod1* and *Cdh23* genotypes on the percent of inner and outer hair cell loss along the entire cochlea and in regions 30%, 50%, and 70% from the cochlear apex. The probabilities of obtaining the calculated F ratios solely by chance are shown for each effect in each cochlear region. Statistically significant effects at the 0.05 alpha level are indicated by a single asterisk and at the 0.001 level by two asterisks. The digenic genotypes for the Tukey pairwise tests of means are indicated by letters as follows: $Sod1^{+/+} Cdh23^{+/+}$ (**A**), $Sod1^{+/+} Cdh23^{ahl/ahl}$ (**B**), $Sod1^{-/-} Cdh23^{+/+}$ (**C**), $Sod1^{-/-} Cdh23^{ahl/ahl}$ (**D**). Only those genotype pairs with significant mean differences at the 0.05 alpha level are shown.

	entire cochlea	30% from Apex	50% from Apex	70% from Apex
Inner Hair Cells				
ANOVA for monogenic genotypes				
Sod1 main effect	0.457	0.620	0.168	0.022 *
Cdh23 main effect	<0.0001 **	0.114	0.071	<0.0001 **
*Sod1*Cdh23* interaction	0.008 *	0.055	0.024 *	0.0004 **
Tukey pairwise tests of digenic genotypes				
significant mean differences (p<0.05)	A-D, B-C, C-D	none	A-C, C-D	A-B, A-C, A-D, B-C, C-D
Outer Hair Cells				
ANOVA for monogenic genotypes				
Sod1 main effect	0.101	0.072	0.048 *	0.141
Cdh23 main effect	<0.0001 **	0.073	<0.0001 **	<0.0001 **
*Sod1*Cdh23* interaction	0.284	0.114	0.536	0.119
Tukey pairwise tests of digenic genotypes				
significant mean differences (p<0.05)	A-B, A-D, B-C, C-D	none	A-B, A-D, B-C, C-D	A-B, A-D, B-C, C-D